

Solid Solutions of Hydrogen Uranyl Phosphate and Hydrogen Uranyl Arsenate. A Family of Luminescent, Lamellar Hosts

Peter K. Dorhout, Guy L. Rosenthal, and Arthur B. Ellis*

Received August 10, 1987

Hydrogen uranyl phosphate, $\text{HfO}_2\text{PO}_4 \cdot 4\text{H}_2\text{O}$ (HUP), and hydrogen uranyl arsenate, $\text{HfO}_2\text{AsO}_4 \cdot 4\text{H}_2\text{O}$ (HUAs), form solid solutions of composition $\text{HfO}_2(\text{PO}_4)_{1-x}(\text{AsO}_4)_x$ (HUPAs), representing a family of lamellar, luminescent solids that can serve as hosts for intercalation chemistry. The solids are prepared by aqueous precipitation reactions from uranyl nitrate and mixtures of phosphoric and arsenic acids; thermogravimetric analysis indicates that the phases are tetrahydrates, like HUP and HUAs. Powder X-ray diffraction data reveal the HUPAs solids to be single phases whose lattice constants increase with X , in rough accord with Vegard's law. Spectral shifts observed for the HUPAs samples in infrared spectra and in electronic absorption and emission spectra are all consistent with the formation of solid solutions. Emission from the solids is efficient (quantum yields of ~ 0.2) and long-lived (lifetimes of $\sim 150 \mu\text{s}$), although the measured values are uniformly smaller than those of HUP and HUAs; unimolecular radiative and nonradiative rate constants for excited-state decay of ~ 1500 and 5000 s^{-1} , respectively, have been calculated for the compounds.

Introduction

The isostructural layered solids hydrogen uranyl phosphate, $\text{HfO}_2\text{PO}_4 \cdot 4\text{H}_2\text{O}$ (HUP), and hydrogen uranyl arsenate, $\text{HfO}_2\text{AsO}_4 \cdot 4\text{H}_2\text{O}$ (HUAs), have proven to be versatile hosts for intercalative ion-exchange reactions.¹⁻³ Both solids exhibit efficient photoluminescence (PL) characteristic of the UO_2^{2+} moiety at room temperature.^{2,4} We have exploited this feature to characterize intercalation reactions and host-guest interactions.⁵⁻⁷

Previous studies have indicated that isostructural compounds such as ZrP_2O_7 and ZrAs_2O_7 form solid solutions of the type $\text{Zr}(\text{P}_2\text{O}_7)_{1-x}(\text{As}_2\text{O}_7)_x$.⁸ It occurred to us that the similarity of HUP and HUAs might permit the preparation of solid solutions of the type $\text{HfO}_2(\text{PO}_4)_{1-x}(\text{AsO}_4)_x$ (HUPAs). Such compounds would be expected to retain the lamellar structure and intense PL of the parent solids, while providing a tunable host structure for intercalation studies. We report herein that these HUPAs phases are readily prepared and comprise a family of luminescent, lamellar host solids.

Experimental Section

Materials. Uranyl nitrate, $\text{UO}_2(\text{NO}_3)_2 \cdot 6\text{H}_2\text{O}$, 99.3%, was supplied by Fisher Scientific, 85% H_3PO_4 by Mallinckrodt, and 99% As_2O_5 by Aldrich. These compounds were used as received. Samples of $\text{HfO}_2(\text{PO}_4)_{1-x}(\text{AsO}_4)_x$ (HUPAs) were prepared from stock solutions (triply distilled water) of 1.0 M $\text{UO}_2(\text{NO}_3)_2$, 1.0 M H_3PO_4 , and 1.0 M H_3AsO_4 , the last prepared by dissolving 11.5 g of As_2O_5 in water, making 100 mL of solution. In a typical synthesis, 20 mL of the $\text{UO}_2(\text{NO}_3)_2$ solution was combined with 5 mL of the H_3PO_4 solution and 15 mL of the H_3AsO_4 solution to yield the solid solution having $X \sim 0.75$ (sample A); 10 mL of each acid solution was used to make the $X \sim 0.50$ solid solution (sample B); and 5 mL of H_3AsO_4 and 15 mL of H_3PO_4 were mixed to yield the $X \sim 0.25$ solid solution (sample C). After mixing, the solutions were vigorously stirred for 2 h at room temperature. The yellow solids that precipitated were filtered, washed five times with 30 mL of triply distilled water, and air-dried for 12 h. Samples of HUP and HUAs were prepared as previously reported.^{1,2} Elemental analyses (Galbraith) indicated that the three samples had compositions of $X = 0.78$, 0.48, and 0.19. Found for A: U, 50.22; P, 1.40; As, 11.79. Found for B: U, 51.73; P, 3.36; As, 7.54. Found for C: U, 53.01; P, 5.48; As, 3.14. Thermogravimetric analyses (TGA) and differential thermal analyses (DTA) were collected on a Netzsch Gerätebau STA 409 thermal analysis system, using a thermal ramp of $5^\circ\text{C}/\text{min}$ from 25 to 500°C . The TGA data gave 4.1, 4.1, and 4.4 waters of hydration for samples A, B, and C, respectively, yielding overall compositions of $\text{HfO}_2(\text{PO}_4)_{0.22}(\text{AsO}_4)_{0.78} \cdot 4.1\text{H}_2\text{O}$, $\text{HfO}_2(\text{PO}_4)_{0.52}(\text{AsO}_4)_{0.48} \cdot 4.1\text{H}_2\text{O}$, and $\text{HfO}_2(\text{PO}_4)_{0.81}(\text{AsO}_4)_{0.19} \cdot 4.4\text{H}_2\text{O}$.

Structure. Powder X-ray diffraction data were collected on a Nicolet 12 rotating-stage powder diffractometer using $\text{Cu K}\alpha$ radiation. The patterns were indexed and the cell constants refined by using least-squares analysis. Similar analyses were performed on pure samples of HUP and HUAs. Diffraction patterns were indexed on the basis of tetragonal unit cells for all the salts. Values of $1/d^2$ and hkl assignments

based on a least-squares analysis are available as supplementary material.

Optical Measurements. Electronic spectra were recorded on a Varian Cary 17-D UV-vis-near-IR spectrophotometer, using silicone grease mulls, as previously reported.² For PL spectra, samples were excited with a Coherent Innova 90 Ar^+ laser; the laser beam was passed through an interference filter to eliminate plasma lines. Emission spectra at 295 K were obtained with a 0.35-m McPherson Model 270 monochromator, a LeCroy Model 4604 photon counter, and a cooled EMI Model 9684B PMT; the spectral resolution was 0.7 nm. The system was controlled with an Apple IIe microprocessor.

Lifetimes and Quantum Yields. Lifetimes were acquired by exciting the samples at 450 nm with a Moletron DL-II tunable dye laser that was pumped by a Moletron UV-12 pulsed N_2 laser; a pulse rate of 20 Hz was employed. The PL signal was fed by an optical fiber into the detection optics of an Aminco-Bowman emission spectrometer, where it was detected at 525 nm by a Hamamatsu 1P21 PMT. Decay curves were monitored with a Tektronix Model 466 oscilloscope, digitized, and evaluated by using the microprocessor; plots of $\log(\text{intensity})$ vs time were linear over at least 2 lifetimes. Quantum yields were measured as described previously.²

Results and Discussion

Powdered samples of $\text{HfO}_2(\text{PO}_4)_{1-x}(\text{AsO}_4)_x$ (HUPAs) are easily prepared and characterized under ambient conditions. In sections below, we describe the synthesis and composition, structure, and optical properties of three such materials.

Synthesis and Composition. The precipitation reaction that produces HUP or HUAs from aqueous uranyl nitrate and phosphoric or arsenic acid affords a straightforward synthetic route to the HUPAs solid solutions. We find that mixing the two acids leads to a solid of stoichiometry comparable to that of the acid mixture. Thus, from solutions targeted to yield solids with $X = 0.25$, 0.50, and 0.75, we isolated powders that had compositions of $X = 0.19$, 0.48, and 0.78.

Hydration plays an important role in defining the physico-chemical properties of HUP and HUAs.^{2,9} Thermogravimetric analyses (TGA) and differential thermal analyses (DTA) were conducted on the HUPAs solids. TGA yielded traces that are similar to those previously reported for HUP and HUAs,^{10,11} indicating the presence of approximately 4 waters of hydration

- (1) Weigel, F.; Hoffmann, G. *J. Less-Common Met.* **1976**, *44*, 99.
- (2) Olken, M. M.; Biagioni, R. N.; Ellis, A. B. *Inorg. Chem.* **1983**, *22*, 4128.
- (3) (a) Pozas-Tormo, R.; Moreno-Real, L.; Martinez-Lara, M.; Bruque-Gomez, S. *Can. J. Chem.* **1986**, *64*, 30. (b) Pozas-Tormo, R.; Moreno-Real, L.; Martinez-Lara, M.; Bruque-Gomez, S. *Inorg. Chem.* **1987**, *26*, 1442.
- (4) Sugitani, Y.; Kato, K.; Nagashima, K. *Bull. Chem. Soc. Jpn.* **1979**, *52*, 918.
- (5) Olken, M. M.; Ellis, A. B. *J. Am. Chem. Soc.* **1984**, *106*, 7468.
- (6) Olken, M. M.; Verschoor, C. M.; Ellis, A. B. *Inorg. Chem.* **1986**, *25*, 80.
- (7) Rosenthal, G. L.; Ellis, A. B. *J. Am. Chem. Soc.* **1987**, *109*, 3157.
- (8) Hubin, R. C. R. *Seances Acad. Sci., Ser. B* **1973**, *273*, 653.
- (9) Johnson, C. M.; Shilton, M. G.; Howe, A. T. *J. Solid State Chem.* **1981**, *37*, 37.
- (10) Barton, H.; Cordfunke, E. H. P. *Thermochim. Acta* **1980**, *40*, 367.
- (11) Pavkovič, N.; Markovič, M. *Radiochim. Acta* **1983**, *34*, 127.

* To whom correspondence should be addressed.

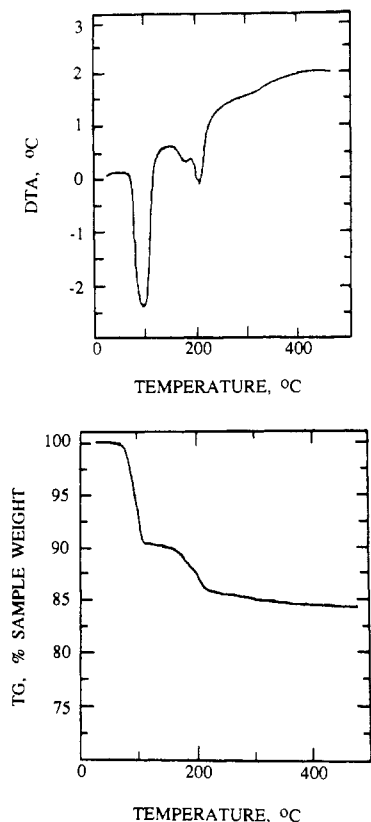


Figure 1. TGA and DTA data for an $\text{H}_2\text{O}_2(\text{PO}_4)_{1-x}(\text{AsO}_4)_x$ sample with $X = 0.48$.

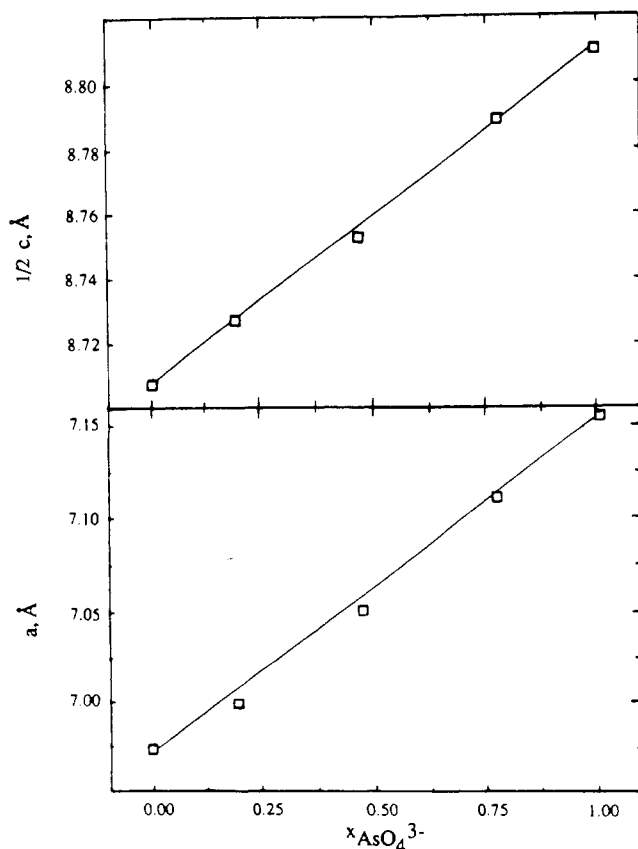


Figure 2. Vegard's law plots of the lattice parameters a and $1/2c$ vs. the mole fraction of arsenate ion in the $\text{H}_2\text{O}_2(\text{PO}_4)_{1-x}(\text{AsO}_4)_x$ family of solids. Lattice parameters from which these plots are derived are given in Table I.

in each sample. Representative plots for the $X = 0.48$ solid are shown in Figure 1. For this sample, roughly 2.4 waters of hy-

Table I. Lattice Constants for $\text{H}_2\text{O}_2(\text{PO}_4)_{1-x}(\text{AsO}_4)_x$ Samples^a

X	a , Å	$1/2c$, Å ^b
0.00 (HUP)	6.973 (3)	8.707 (5)
0.19	6.999 (2)	8.727 (3)
0.48	7.051 (2)	8.751 (3)
0.78	7.110 (1)	8.789 (2)
1.00 (HUAs)	7.157 (1)	8.806 (2)

^a All samples were single phases that could be indexed to tetragonal unit cells. Errors in table entries are estimated standard deviations based on least-squares refinement. ^b The $1/2c$ lattice parameter represents the interlamellar spacing, viz., the interplanar spacing between adjacent uranyl-phosphate-arsenate layers.¹²

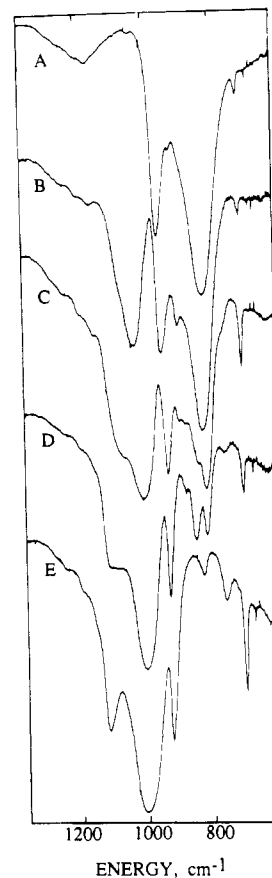


Figure 3. IR spectra of $\text{H}_2\text{O}_2(\text{PO}_4)_{1-x}(\text{AsO}_4)_x$ samples with $X = 1.00$ (HUAs), 0.78, 0.48, 0.19, and 0.00 (HUP), curves A, B, C, D, and E, respectively. All spectra were obtained at 295 K with the use of KBr pellets.

dration are lost near 100 °C and an additional 1.7 waters are lost from 160 to 400 °C.

Structure. Convincing evidence that solid solutions have been prepared is provided by X-ray powder diffraction data. Both HUP and HUAs are lamellar solids whose powder patterns can be indexed in tetragonal symmetry.^{12,13} The X-ray diffraction data obtained for the HUPAs solids indicate them to be single phases whose patterns can also be indexed in tetragonal symmetry, with $1/2c$ corresponding to the interlamellar spacing. Table I presents the lattice constants derived from X-ray data. Both a and $1/2c$ are seen to increase with X . A graphic presentation of these data, shown in Figure 2, indicates good agreement with Vegard's law: the lattice constants vary roughly linearly with composition.¹⁴

Infrared spectra of the HUPAs solids differ from those of physical mixtures of HUP and HUAs matched to the same composition, providing additional evidence for the new phases.

- (12) Morosin, B. *Acta Crystallogr. Sect. B: Struct. Crystallogr. Cryst. Chem.* **1978**, *B34*, 3732.
 (13) Shilton, M. G.; Howe, A. T. *J. Solid State Chem.* **1980**, *34*, 137.
 (14) Pearson, W. B. *The Crystal Chemistry and Physics of Metals and Alloys*; Wiley: New York, 1972; pp 174-176.

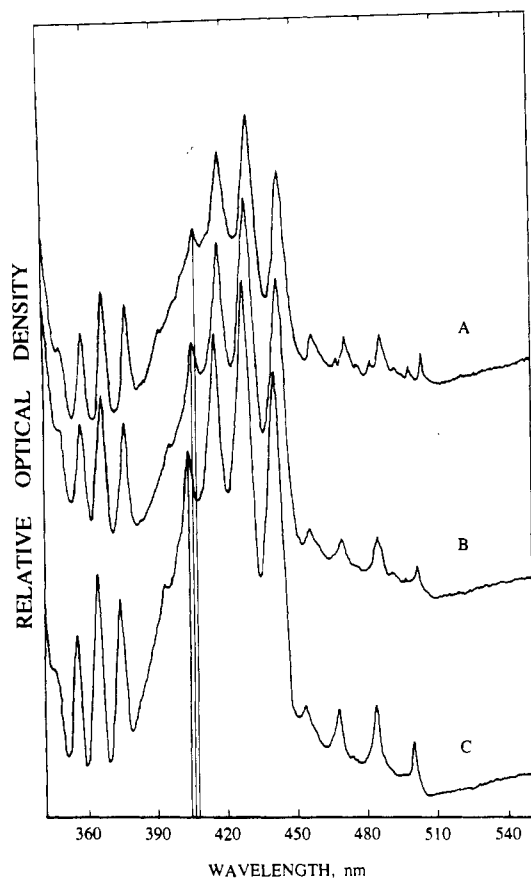


Figure 4. Visible absorption spectra (295 K) of $\text{HUO}_2(\text{PO}_4)_{1-x}(\text{AsO}_4)_x$ samples, recorded as silicone grease mulls on filter paper with silicone grease on paper serving as a reference. Shown are spectra for samples with $X = 1.00$ (HUAs), 0.48, and 0.00 (HUP), curves A, B, and C, respectively. Vertical lines are included to highlight spectral shifts.

Figure 3 compares the HUPAs spectra with those of the parent HUP and HUAs solids. Dominating the spectra are stretching modes due to the phosphate and arsenate moieties at ~ 1000 and 810 cm^{-1} , respectively;^{15,16} their relative intensities vary as expected as the phosphate-to-arsenate ratio changes. We also observe that the HUP ν_3 phosphate stretching bands¹⁶ at 1120 and 1000 cm^{-1} move toward one another as X increases. Another noteworthy trend in the spectra is the gradual shift of the strong sharp band due to the UO_2^{2+} asymmetric stretching mode:¹⁵ the band is found at $945, 938, 928, 925,$ and 923 cm^{-1} as X takes on values of 1.00 (HUAs), $0.78, 0.48, 0.19,$ and 0.00 (HUP). This result accords with previous studies that demonstrated the sensitivity of this vibrational mode to environment.¹⁷

Optical Properties. The HUPAs phases, like HUP and HUAs, are yellow. Electronic absorption spectra of all of the solids are dominated by the vibrationally structured bands characteristic of the UO_2^{2+} moiety. Figure 4 presents spectra for samples with $X = 1.00$ (HUAs), $0.48,$ and 0.00 (HUP). It is clear from the figure that the $X = 0.48$ spectrum is not derived by superimposing HUP and HUAs spectra, as would be the case for a physical mixture, but rather is composed of bands that fall between those of the parent solids. The overall red shift in corresponding band maxima in passing from HUP to HUAs is $\sim 100\text{ cm}^{-1}$. Although not shown in Figure 4, the spectral envelopes for the $X = 0.19$ and 0.78 samples are bracketed, as expected, by the $X = 0.48$ sample and HUP and HUAs, respectively.

As noted in the Introduction, HUP and HUAs exhibit yellow-green PL characteristic of the UO_2^{2+} moiety when irradiated

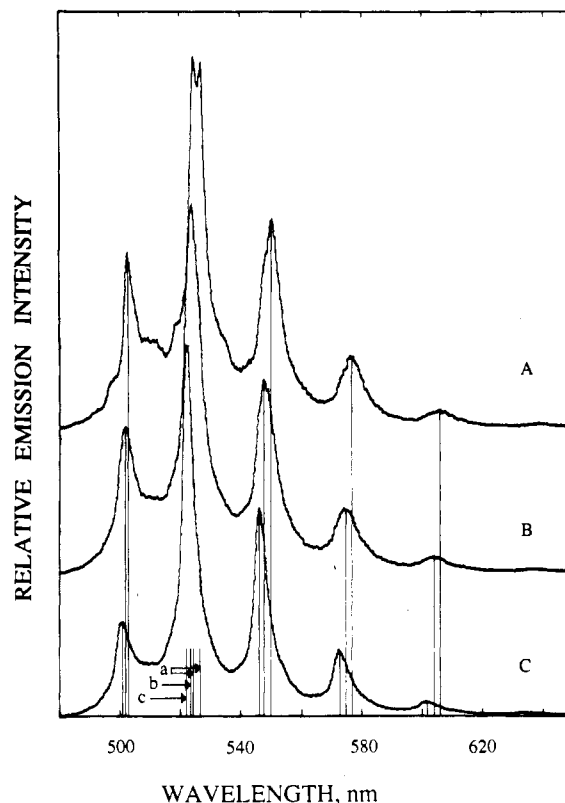


Figure 5. Emission spectra (295 K) of $\text{HUO}_2(\text{PO}_4)_{1-x}(\text{AsO}_4)_x$ samples with $X = 1.00$ (HUAs), 0.48, and 0.00 (HUP), curves A, B, and C, respectively. All samples were excited with 457.9-nm light. Vertical lines are included to highlight spectral shifts. Positions of peaks near 525 nm are indicated with lower-case letters.

Table II. Emissive Properties of $\text{HUO}_2(\text{PO}_4)_{1-x}(\text{AsO}_4)_x$ Samples^a

X	ϕ_r^b	$\tau, \mu\text{s}^c$	$10^{-3}k_r^d, \text{s}^{-1}$	$10^{-3}k_{nr}^e, \text{s}^{-1}$
0.00 (HUP)	0.70	450	1.5	0.70
0.19	0.16	130	1.2	6.5
0.48	0.25	160	1.6	4.7
0.78	0.20	160	1.3	5.0
1.00 (HUAs)	0.50	230	2.1	2.2

^a Emissive data were obtained at 295 K. ^b Radiative quantum efficiency was obtained with 450-nm excitation, as described in the Experimental Section. Errors in these values have been estimated to be $\pm 25\%$.¹⁸ ^c Measured lifetimes were obtained with 450-nm excitation, as described in the Experimental Section. ^d Unimolecular radiative rate constant, calculated by using eq 1 in the text. ^e Unimolecular nonradiative rate constant, calculated by using eq 2 in the text.

with blue or near-UV light. The PL counterparts of the absorption spectra of Figure 4 are shown in Figure 5; although the data presented were obtained with 457.9-nm excitation, other Ar^+ laser lines ($472.7, 476.5, 488.0,$ and 496.5 nm) yielded identical spectra. The structured PL spectra of Figure 5 parallel the absorption spectra in displaying a red shift with increasing AsO_4^{3-} content; an overall shift of $\sim 100\text{ cm}^{-1}$ in passing from HUP to HUAs is common to the absorption and PL spectra and has been observed previously in PL measurements.⁴ The PL spectra of the solid solutions fall regularly between the compositional extremes, as illustrated for the $X = 0.48$ sample in Figure 5.

Besides spectral distributions, the solid-solution PL quantum yields, ϕ_r , and lifetimes, τ , of the new phases are of interest. Because the HUPAs phases, like HUP and HUAs, exhibit simple unimolecular decay, the first-order radiative and nonradiative rate constants k_r and k_{nr} can be calculated from eq 1 and 2; in terms

$$k_r = \phi_r / \tau \quad (1)$$

$$k_{nr} = (1/\tau) - k_r \quad (2)$$

of these rate constants, $\tau = (k_r + k_{nr})^{-1}$ and $\phi_r = k_r(k_r + k_{nr})^{-1}$. Values of ϕ_r and τ , along with calculated values of k_r and k_{nr} , are

(15) Pekárek, V.; Vesely, V. *J. Inorg. Nucl. Chem.* **1965**, *27*, 1151.
 (16) Pham-Thi, M.; Colomban, Ph. *J. Less-Common Met.* **1985**, *108*, 189.
 (17) (a) Nakamoto, K. *Infrared and Raman Spectra of Inorganic and Coordination Compounds*, 3rd ed.; Wiley: New York, 1978; p 115. (b) Ohwada, K. *Spectrochim. Acta, Part A* **1968**, *24A*, 595.

presented in Table II. The data presented indicate that while the solid solutions are efficient, long-lived emissive hosts ($\phi_r \sim 0.2$; $\tau \sim 150 \mu\text{s}$), they are somewhat less so than HUAs and HUP. In making this statement, we believe it is worth emphasizing that dehydration, which can reduce the PL intensity and lifetime of all these samples, may affect these comparisons. On the other hand, the HUPAs samples all seem to have similar properties, and we expect that the less uniform environment that emitting UO_2^{2+} moieties will see in the HUPAs samples might well promote nonradiative processes. As Table II indicates, k_r values are within a factor of 2 for all the samples examined, whereas k_{nr} decreases by factors of up to 3 and 10 in passing from the solid solutions to HUAs and HUP, respectively.

Conclusion

We have shown in this paper that HUP and HUAs are miscible,

yielding the $\text{H}_2\text{O}_2(\text{PO}_4)_{1-x}(\text{AsO}_4)_x$ (HUPAs) family of luminescent layered solids. With the rich intercalation chemistry that HUP and HUAs possess, the HUPAs solids represent an emissive host system with tunable lattice parameters than can be used to optically and structurally monitor intercalation reactions and host-guest interactions.

Acknowledgment. We are grateful to the Office of Naval Research for generous support of this work. We also thank Quynin Xu for assistance with the TGA and DTA analyses and Drs. M. Markovič and L. F. Dahl for their helpful comments.

Registry No. $\text{UO}_2(\text{NO}_3)_2$, 10102-06-4; H_3PO_4 , 7664-38-2; H_3AsO_4 , 7778-39-4; $\text{H}_2\text{O}_2(\text{PO}_4)_{0.22}(\text{AsO}_4)_{0.78} \cdot 4\text{H}_2\text{O}$, 113160-03-5; $\text{H}_2\text{O}_2(\text{PO}_4)_{0.52}(\text{AsO}_4)_{0.48} \cdot 4\text{H}_2\text{O}$, 113160-05-7; $\text{H}_2\text{O}_2(\text{PO}_4)_{0.81}(\text{AsO}_4)_{0.19} \cdot 4\text{H}_2\text{O}$, 113160-07-9.

Supplementary Material Available: Listings of $1/d^2$ values and hkl assignments (7 pages). Ordering information is given on any current masthead page.

(18) Wrighton, M. S.; Ginley, D. S.; Morse, D. L. *J. Phys. Chem.* **1974**, *78*, 2229.

Contribution from the School of Chemical Sciences, University of Georgia, Athens, Georgia 30602, Departamento de Quimica, Universidad Nacional de Colombia, Bogota, Colombia, and Centro de Quimica Estrutural, Universidade Nova de Lisboa, 1000 Lisbon, Portugal

Electronic and Magnetic Properties of Nickel-Substituted Rubredoxin: A Variable-Temperature Magnetic Circular Dichroism Study

Andrzej T. Kowal,^{1a} Isabel C. Zambrano,^{1b} Isabel Moura,^{1c} Jose J. G. Moura,^{1c} Jean LeGall,^{1a} and Michael K. Johnson*^{1a}

Received August 26, 1987

Ni(II)-substituted rubredoxins from *Desulfovibrio gigas*, *Desulfovibrio vulgaris*, and *Clostridium pasteurianum* have been prepared and characterized by room-temperature UV-visible absorption and low-temperature MCD spectroscopy. The results are compared with those obtained for the crystallographically defined analogue complex $(\text{Ph}_4\text{P})_2\text{Ni}(\text{SPh})_4$. The Ni(II) sites in both the biological and inorganic compounds are found to be high spin, with very similar electronic and magnetic properties. The results are interpreted in terms of tetragonally distorted tetrahedral thiolate coordination for Ni(II), resulting in a $^3\text{A}_2$ ground state, under D_{2d} symmetry, that is subject to large axial zero-field splitting. Studies of the temperature dependence of the solution MCD spectra facilitate quantitative assessment of the axial zero-field splitting parameters; $D = 55 \text{ cm}^{-1}$ for Ni(II)-substituted Rd and $D = 44 \text{ cm}^{-1}$ for $\text{Ni}(\text{SPh})_4^{2-}$. The properties of Ni(II) sites in hydrogenases are discussed in light of these results.

Introduction

Nickel has recently been shown to be present in at least four distinct types of biological systems:^{2,3} urease from plant cells; hydrogenases from sulfate-reducing, methanogenic, photosynthetic, nitrogen-fixing, and "Knallgas" bacteria; CO dehydrogenase from acetogenic bacteria; a low molecular weight tetrapyrrole prosthetic group, factor F_{430} , which is present in methanogenic bacteria. In each instance the available spectroscopic data indicate that the nickel has a unique coordination environment. For hydrogenases EXAFS,⁴⁻⁶ EPR,⁷ and MCD⁸ spectroscopies have provided evi-

dence for sulfur coordination of a monomeric nickel center in the oxidized enzymes. However, there are presently few monomeric nickel thiolate complexes that could serve as model compounds and thereby facilitate detailed characterization of the ligand environment and coordination geometry.

In this work, we report spectroscopic investigations of nickel substituted rubredoxins, in which monomeric Ni(II) is ligated by four cysteinyl sulfur atoms. The electronic and magnetic properties of the Ni-substituted rubredoxins and the structurally well-characterized analogue complex $(\text{Ph}_4\text{P})_2\text{Ni}(\text{SPh})_4$ ^{9,10} have been investigated by UV-visible adsorption and variable-temperature MCD spectroscopies. The results indicate tetragonally distorted tetrahedral nickel thiolate coordination and provide insight into the nature and magnitude of the splitting of the electronic ground state. The coordination of nickel in hydrogenases is discussed in the light of these results.

Experimental Section

Preparation of Compounds. Rubredoxin (Rd) was purified to homogeneity from *Desulfovibrio gigas*, *Desulfovibrio vulgaris*, and *Clostridium pasteurianum* by using the published procedures.¹¹ The experi-

- (1) (a) University of Georgia. (b) Universidad Nacional de Colombia. (c) Universidade Nova de Lisboa.
- (2) Thauer, R. K.; Diekert, G.; Schönheit, P. *Trends Biochem. Sci. (Pers. Ed.)* **1980**, *11*, 304.
- (3) Thomson, A. J. *Nature (London)* **1982**, *298*, 602.
- (4) Lindahl, P. A.; Kojima, R. P.; Hausinger, R. P.; Fox, J. A.; Teo, B. K.; Walsh, C. T.; Orme-Johnson, W. H. *J. Am. Chem. Soc.* **1984**, *106*, 3062.
- (5) Scott, R. A.; Wallin, S. A.; Czechowski, M.; DerVartanian, D. V.; LeGall, J.; Peck, H. D., Jr.; Moura, I. *J. Am. Chem. Soc.* **1984**, *106*, 6864.
- (6) Scott, R. A.; Czechowski, M.; DerVartanian, D. V.; LeGall, J.; Peck, H. D., Jr.; Moura, I. *Rev. Port. Quim.* **1985**, *27*, 67.
- (7) Albracht, S. P. J.; Kröger, A.; Van der Zwaan, J. W.; Unden, G.; Böcher, R.; Mell, H.; Fontijn, R. D. *Biochim. Biophys. Acta* **1986**, *874*, 116.
- (8) Johnson, M. K.; Zambrano, I. C.; Czechowski, M. H.; Peck, H. D., Jr.; DerVartanian, D. V.; LeGall, J. *Biochem. Biophys. Res. Commun.* **1985**, *128*, 220.

- (9) Holah, D. G.; Coucouvanis, D. *J. Am. Chem. Soc.* **1975**, *97*, 6917.
- (10) Swenson, D.; Baenziger, N. C.; Coucouvanis, D. *J. Am. Chem. Soc.* **1978**, *100*, 1932.
- (11) (a) Moura, I.; Bruschi, M.; LeGall, J.; Moura, J. J. G.; Xavier, A. V. *Biochem. Biophys. Res. Commun.* **1977**, *75*, 1037. (b) Bruschi, M.; LeGall, J. *Biochim. Biophys. Acta* **1972**, *263*, 279. (c) Lovenberg, W. *Methods Enzymol.* **1971**, *24*, 477.